

General Analysis of B Meson Decay into Two Fermions

Akihiro Matsuzaki¹

*Department of Physics, Rikkyo University,
Nishi-ikebukuro, Toshima-ku Tokyo, Japan, 171*

Abstract

We study how to measure the current structure of the process that B meson decays into two unstable fermions \bar{f}_a and f_b in model independent way. We use the momentum distributions of subsequent decay products affected by $\bar{f}_a f_b$ spin correlation. We have found the following: (1) We can extract the absolute values of two effective coupling constants from the opening angle between the particles decayed from \bar{f}_a and f_b . (2) We can extract the real part of the interference from the energy distribution of one of the decayed particles from \bar{f}_a or f_b . (3) No new information can be obtained from the energy distribution of two decayed particles from \bar{f}_a and f_b . (4) The imaginary part of interference is extracted from the azimuthal angle asymmetry of final-state decay products. (5) If only one of two fermions is unstable, we can extract the real part of interference from each of the energy distribution and opening angle distribution. We show several simple examples.

¹akihiro@rikkyo.ac.jp

1 Introduction

A huge number of B mesons are produced in B-factories. They are used to confirm the Standard Model (SM). Almost of all the results suggest that the SM, and especially, Kobayashi-Mazkawa ansatz are reliable. Recently, we search for rare events and SM-forbidden phenomena in B-factories with high statistics. However, new physics has not been seen.

To discover them, it is important to search through many modes and many physical quantities. They are, for instance, CP asymmetry, forward-backward asymmetry, left-right asymmetry, energy distribution, and angular distribution. We want to detect not only the decay width but also these quantities. Also, we want to analyze as many channels as possible using the unified form for simplicity, facility, and practicality. Another important thing to discover the new physics is making the reliable SM prediction especially for the non-perturbative QCD effect. Also for this purpose, determining many physical quantities is significant.

In this paper, we consider the general $B \rightarrow \bar{f}_a f_b$ decay modes, where f_a and f_b are arbitrary fermions and \bar{f}_a is the antiparticle of f_a . The CP violation can be measured in some of these modes [1]. These modes can be divided in two types. One is the leptonic decay modes and another is the baryonic decay modes. The SM prediction in leptonic modes are [2, 3]

$$\begin{aligned} Br(B_d^0 \rightarrow \tau^+ \tau^-) &\simeq 2.8 \times 10^{-8} \\ Br(B_s^0 \rightarrow \tau^+ \tau^-) &\simeq 8.9 \times 10^{-7}. \end{aligned} \quad (1)$$

The experimental upper bound is [4]

$$Br(B_d^0 \rightarrow \tau^+ \tau^-) < 4.1 \times 10^{-3}. \quad (2)$$

On the other hand, the branching ratios of baryonic modes are predicted as [5]

$$\begin{aligned} Br(B_d^0 \rightarrow \bar{\Xi}_c^- \Lambda_c^+) &\sim 2.0 \times 10^{-3} \\ Br(B_u^+ \rightarrow \bar{\Xi}_c^0 \Lambda_c^+) &\sim 2.2 \times 10^{-3}. \end{aligned} \quad (3)$$

The experimental upper bounds are for example, [4]

$$\begin{aligned} Br(B_d^0 \rightarrow \Delta^0 \bar{\Lambda}) &< 9.3 \times 10^{-7} \\ Br(B_d^0 \rightarrow \bar{\Lambda} \Lambda) &< 3.2 \times 10^{-7} \\ Br(B_d^0 \rightarrow \bar{\Lambda}_c^- p) &= (2.1_{-0.5}^{+0.7}) \times 10^{-5} \\ Br(B_d^0 \rightarrow \bar{\Lambda}_c^- \Lambda_c^+) &< 6.2 \times 10^{-5}, \end{aligned} \quad (4)$$

$$\begin{aligned} Br(B_u^+ \rightarrow \Delta^+ \bar{\Lambda}) &< 8.2 \times 10^{-7} \\ Br(B_u^+ \rightarrow \bar{\Xi}_c^0 \Lambda_c^+) Br(\bar{\Xi}_c^0 \rightarrow \bar{\Xi}^+ \pi^-) &= (5.6_{-2.4}^{+2.7}) \times 10^{-5} \\ Br(B_u^+ \rightarrow \bar{\Xi}_c^0 \Lambda_c^+) Br(\bar{\Xi}_c^0 \rightarrow K^+ \pi^-) &= (4.0 \pm 1.6) \times 10^{-5}. \end{aligned}$$

$B_d^0 \rightarrow \bar{\Lambda}_c^- p$ and $B_u^+ \rightarrow \Xi_c^0 \Lambda_c^+$ have already been seen. Also, some other modes are predicted to be seen in near future by the SM or other models. Comparing the experimental result with the model predictions of current structure, we try to discover new physics, select a reasonable model, and consider the non-perturbative QCD effects.

The modes which decay into unstable particles decrease the efficiency since it is difficult to detect the events, however these modes have the advantage in correlation detection. The correlation is detected as momentum distribution of a and b , which are the decay products of \bar{f}_a and f_b , respectively. When we deal with these modes, we have to consider the whole process of

$$\begin{aligned} B &\rightarrow \bar{f}_a + f_b \rightarrow b + \text{anything} \\ &\quad \quad \quad \searrow \\ &\quad \quad \quad \rightarrow a + \text{anything} \end{aligned} \quad (5)$$

because we cannot detect the intermediate state $\bar{f}_a + f_b$.

1.1 $B_q \rightarrow \bar{f}_a f_b$ decay

From the partially conserved axial current relation, the general $B_q \rightarrow \bar{f}_a f_b$ decay amplitude is given by [2]

$$A_q = i f_B m_B G_F [(C_P^q + \frac{m_b + m_a}{m_B} C_A^q)(\bar{f}_b \gamma_5 f_a) + (C_S^q + \frac{m_b - m_a}{m_B} C_V^q)(\bar{f}_b f_a)], \quad (6)$$

where f_B , m_B , and G_F are B meson decay constant, B meson mass, and the Fermi constant, respectively; m_a and m_b are \bar{f}_a and f_b masses, respectively; C_P^q , C_S^q , C_A^q , and C_V^q are the complex coefficients of pseudo scalar, scalar, axial, and vector currents, respectively; The superscript q represents the valence u , d , s or c quark in B meson.

In charged B meson decays, we simply set

$$\begin{aligned} C_1 &\equiv C_P^q + \frac{m_b + m_a}{m_B} C_A^q \\ C_2 &\equiv C_S^q + \frac{m_b - m_a}{m_B} C_V^q. \end{aligned} \quad (7)$$

On the other hand, in neutral B meson decays, considering the $B^0 - \bar{B}^0$ mixing effect, we set [6]-[8]

$$\begin{aligned} |B^0(t)\rangle &= g_+(t)|B^0\rangle + \frac{q}{p}g_-(t)|\bar{B}^0\rangle, \\ g_{\pm}(t) &= \frac{1}{2}e^{-im_B t}e^{-\frac{1}{2}\Gamma_B t}\left[1 \pm e^{-i\Delta m_B t}e^{\frac{1}{2}\Delta\Gamma_B t}\right], \end{aligned} \quad (8)$$

where; t is the time started when B^0 is created; q/p is the ratio of \bar{B}^0 to B^0 in B^0 mass eigenstate; Γ_B is the B^0 total decay width; Δm_B and $\Delta\Gamma_B$ are

the mass difference and decay width difference between heavier and lighter B^0 mesons; Hence, the time dependent effective amplitude takes the form

$$A_q(t) = if_B m_B G_F \left[\tilde{C}_1(\bar{f}_b \gamma_5 f_a) + \tilde{C}_2(\bar{f}_b f_a) \right], \quad (9)$$

where

$$\begin{aligned} \tilde{C}_1 &\equiv \left\{ g_+(t) C_1 + \frac{q}{p} g_-(t) \bar{C}_1 \right\}, \\ \tilde{C}_2 &\equiv \left\{ g_+(t) C_2 + \frac{q}{p} g_-(t) \bar{C}_2 \right\}. \end{aligned} \quad (10)$$

These parameters appear in the differential decay width in the form of $|\tilde{C}_1|^2$, $|\tilde{C}_2|^2$, $Re[\tilde{C}_1 \tilde{C}_2^*]$, and $Im[\tilde{C}_1 \tilde{C}_2^*]$. These quantities depend on the decay time. However, for $|p/q| = |C_1/\bar{C}_1| = |C_2/\bar{C}_2| = 1$ and $\Delta\Gamma_B = 0$, integrating over the time and summing over B^0 decays and \bar{B}^0 decays, these quantities becomes $2|C_1|^2/\Gamma_B$, $2|C_2|^2/\Gamma_B$, $(Re[C_1 C_2^*] + Re[\bar{C}_1 \bar{C}_2^*])/\Gamma_B$, and $(Im[C_1 C_2^*] + Im[\bar{C}_1 \bar{C}_2^*])/\Gamma_B$, respectively. Hence, we omit the time dependence and the tildes on C_1 and C_2 in most of the rest of this paper.

We want to give the $B \rightarrow \bar{f}_a f_b$ partial decay width in which \bar{f}_a and f_b have particular polarizations. Thus, we introduce the polarization vectors s^a and s^b of \bar{f}_a and f_b , respectively. These vectors have the constraints $(s^a)^2 = (s^b)^2 = -1$ and $s^a \cdot k_{f_a} = s^b \cdot k_{f_b} = 0$, where k_{f_a} and k_{f_b} are \bar{f}_a and f_b momenta, respectively.

In B rest frame, the differential decay width of $B \rightarrow \bar{f}_a(s^a) f_b(s^b)$ is given by

$$\begin{aligned} \frac{d\Gamma}{d\Omega} = \frac{f_B^2 G_F^2}{32\pi^2} |\mathbf{p}| &\left\{ D_1 + D_2(s_x^a s_x^b + s_y^a s_y^b) + D_3 s_z^a s_z^b \right. \\ &\left. + D_4\left(\frac{m_b}{m_a} s_z^a - \frac{m_a}{m_b} s_z^b\right) + D_5(s_x^a s_y^b - s_x^b s_y^a) \right\}, \end{aligned} \quad (11)$$

where

$$\begin{aligned} |\mathbf{p}| &= \frac{\sqrt{(m_B^2 - (m_a - m_b)^2)(m_B^2 - (m_a + m_b)^2)}}{2m_B}, \\ D_1 &= |C_1|^2 \frac{m_B^2 - (m_a - m_b)^2}{2} + |C_2|^2 \frac{m_B^2 - (m_a + m_b)^2}{2}, \\ D_2 &= -|C_1|^2 \frac{m_B^2 - (m_a - m_b)^2}{2} + |C_2|^2 \frac{m_B^2 - (m_a + m_b)^2}{2}, \\ D_3 &= -D_1, \\ D_4 &= -2Re[C_1 C_2^*] m_a m_b \gamma_a \gamma_b (\beta_a + \beta_b), \\ D_5 &= -2Im[C_1 C_2^*] m_a m_b \gamma_a \gamma_b (\beta_a + \beta_b), \end{aligned} \quad (12)$$

$$\begin{aligned} \beta_a &\equiv \frac{|\mathbf{k}_{f_a}|}{k_{f_a}^0}, & \gamma_a &\equiv \frac{1}{\sqrt{1 - \beta_a^2}} = \frac{k_{f_a}^0}{m_a}, \\ \beta_b &\equiv \frac{|\mathbf{k}_{f_b}|}{k_{f_b}^0}, & \gamma_b &\equiv \frac{1}{\sqrt{1 - \beta_b^2}} = \frac{k_{f_b}^0}{m_b}, \end{aligned} \quad (13)$$

and Ω is the solid angle of k_{f_a} .

The general $B \rightarrow \bar{f}_a f_b \rightarrow a + b + \text{anything}$ differential decay width is written as

$$\begin{aligned} \frac{d\Gamma}{d\Omega d^3k_a d^3k_b} = \sum_{s^a, s^b} \sum_{\pm s^a, \pm s^b} & \frac{d\Gamma(B \rightarrow \bar{f}_a(s^a) f_b(s^b))}{dt d\Omega} \\ & \times \frac{dBr(\bar{f}_a(s^a) \rightarrow a + \text{anything})}{d^3k_a} \\ & \times \frac{dBr(f_b(s^b) \rightarrow b + \text{anything})}{d^3k_b}, \end{aligned} \quad (14)$$

where \sum implies sum over polarizations. k_a and k_b are the momenta of the particle a and b in \bar{f}_a and f_b rest frame, respectively. The differential branching ratios of \bar{f}_a and f_b are written in Appendix A.

In writing the explicit form of the decay width, we will use the following notation (See Fig. 1.): In B rest frame, \bar{f}_a is oriented in the positive z -axis direction. The zenith angles of a and b directions in B rest frame are θ_a and θ_b , respectively. The azimuthal angle between a and b directions is ϕ . d_z is the distance between \bar{f}_a and f_b decay points.

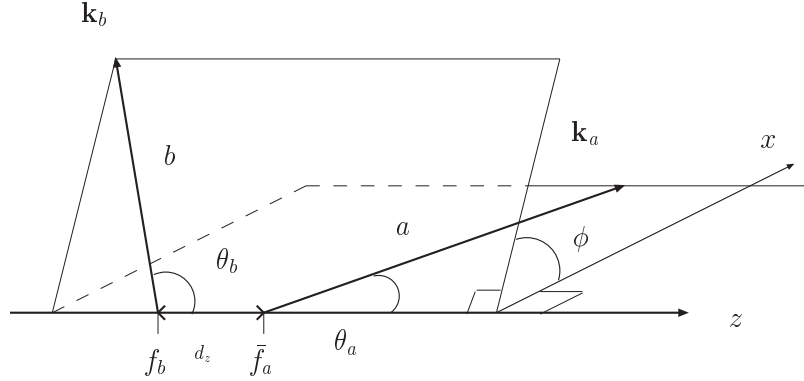


Figure 1: B meson rest frame. \bar{f}_a is oriented in the positive z -axis direction. The zenith angles of a and b directions are θ_a and θ_b , respectively. The azimuthal angle between a and b is ϕ . The distance between \bar{f}_a and f_b decay points is d_z . a and b have the momenta k_a and k_b , respectively.

In the massless limit of a and b , we obtain the general formula

$$\begin{aligned}
& \frac{d\Gamma}{dy_a d\Omega_a dy_b d\Omega_b} \\
&= Br_a \frac{y_a^2}{4\pi\lambda_a} Br_b \frac{y_b^2}{4\pi\lambda_b} \frac{f_B^2 G_F^2}{2\pi} |\mathbf{p}| \\
& \times \left[D_1 G_1^a(y_a) G_1^b(y_b) + D_4 \left\{ \frac{m_b}{m_a} \cos\theta_a G_1^b(y_b) G_2^a(y_a) + \frac{m_a}{m_b} \cos\theta_b G_1^a(y_a) G_2^b(y_b) \right\} \right. \\
& \quad \left. - (D_2 \sin\theta_a \sin\theta_b \cos\phi - D_1 \cos\theta_a \cos\theta_b + D_5 \sin\theta_a \sin\theta_b \sin\phi) G_2^a(y_a) G_2^b(y_b) \right], \tag{15}
\end{aligned}$$

where

$$\begin{aligned}
Br_a &= Br(\bar{f}_a \rightarrow a + \text{anything}), \\
Br_b &= Br(f_b \rightarrow b + \text{anything}), \\
y_a &= \frac{2E_a}{m_a}, \quad y_b = \frac{2E_b}{m_b}, \tag{16}
\end{aligned}$$

where E_a and E_b are a and b energy in \bar{f}_a and f_b rest frames, respectively; $G_{1,2}^{a,b}(y_{a,b})$ are the functions which are defined in Appendix A. The massless condition of particles a and b are reasonable because most of τ decay into μ , e , or pions, and substantial unstable baryons decay into a lighter baryon and pions, photons, and/or leptons. They have at most about 100 MeV masses, which are enough smaller than the masses of τ and any baryons.

Using the general formula (15), we first derive the partial decay width. Integrating over $dy_a d\Omega_a dy_b d\Omega_b$, we have

$$\Gamma = Br_a Br_b \frac{f_B^2 G_F^2}{2\pi} |\mathbf{p}| D_1. \tag{17}$$

This width contains the factor D_1 . We determine this coefficient, first. However, we want to know the relation between $|C_1|$ and $|C_2|$. Moreover, we want to know how is the relative phase between C_1 and C_2 . That is what we will do in this paper.

This paper is organized as follows: In Section 2, we consider the energy distribution of a to determine $Re[C_1 C_2^*]$. In Section 3, we consider the distribution of opening angle between a and b to determine $|C_1|$ and $|C_2|$, separately. In Section 4, we consider the azimuthal angle asymmetry of a and b to determine $Im[C_1 C_2^*]$. In Section 5, we discuss the case that f_b is a stable fermion. In Section 6, we show some examples of baryonic mode. In Section 7, we summarize our analysis.

2 Energy Distribution

In this section, we study the energy distribution of the final-state particle a or b . For definiteness, let's say that we want to investigate the a energy distribution.

The prescription to derive the energy distribution formula in B rest frame is as follows [9]: First, we multiply the delta function $\delta(x_a - y_a(1 + \beta_a \cos \theta_a)/2)$ by Eq. (15), where $x_a = E'_a/E_{f_a}$, and E_{f_a} and E'_a are \bar{f}_a and a energy in B rest frame, respectively. x_a means a normalized energy of particle a in B rest frame. Next, we integrate over $dy_a d\Omega_a dy_b d\Omega_b$. Then, we have

$$\frac{1}{\Gamma} \frac{d\Gamma}{dx_a} = \int dy_a \frac{1}{\beta_a \lambda_a} \left\{ y_a G_1^a(y_a) + \frac{D_4}{D_1} \frac{m_b}{m_a \beta_a} (2x_a - y_a) G_2^a(y_a) \right\}. \quad (18)$$

Here, $\int dy_a$ means

$$\int dy_a = \int_{\frac{2x_a}{1+\beta_a}}^{\frac{2x_a}{1-\beta_a}} dy_a \theta[x_a] \theta\left[\frac{1-\beta_a}{2} - x_a\right] + \int_{\frac{2x_a}{1+\beta_a}}^1 dy_a \theta\left[x_a - \frac{1-\beta_a}{2}\right] \theta\left[\frac{1+\beta_a}{2} - x_a\right]. \quad (19)$$

The expression (18) suggests that a energy dependence can be used to determine the coefficient D_4 , which contains $Re[C_1 C_2^*]$. We note that b energy dependence can also be used to determine D_4 , similarly. However, no new information is obtained by the energy distributions of both of a and b , namely, $d\Gamma/(dx_a dx_b)$. This is because D_2 and D_5 terms in the general formula (15) vanish when we integrate over the azimuthal angle ϕ .

2.1 Example 1 - τ^+ Decays into $\mu^+ \nu_\mu \bar{\nu}_\tau$

As a simple example, we calculate μ^+ energy distribution of

$$\begin{aligned} B^0 &\rightarrow \tau^+ + \tau^- \\ &\hookrightarrow \mu^+ + \nu_\mu + \bar{\nu}_\tau. \end{aligned} \quad (20)$$

In this case, we can set $G_1^a(y_a) = 3 - 2y_\mu$, $G_2^a(y_a) = 2y_\mu - 1$, $\lambda_a = \lambda_b = \frac{1}{2}$, and $\beta_a = \beta_b = \sqrt{1 - 4m_\tau^2/m_B^2} \equiv \beta$. Hence, we have

$$\begin{aligned}
& \frac{1}{\Gamma} \frac{d\Gamma}{dx_\mu} \\
&= \frac{2}{\beta} \left[\left\{ \frac{8\beta x_\mu^2 (9(1 - \beta^2) - 4(3 + \beta^2)x_\mu)}{3(1 - \beta^2)^3} \right. \right. \\
&\quad + \frac{2\text{Re}[\tilde{C}_1\tilde{C}_2^*]}{|\tilde{C}_1|^2 + |\tilde{C}_2|^2\beta^2} \frac{8\beta^3 x_\mu^2 (16x_\mu - 3(1 - \beta^2))}{3(1 - \beta^2)^3} \left. \right\} \theta[x_\mu] \theta[\frac{1 - \beta}{2} - x_\mu] \\
&\quad + \left\{ \frac{5(1 + \beta)^3 - 4(9(1 + \beta) - 8x_\mu)x_\mu^2}{6(1 + \beta)^3} \right. \\
&\quad + \frac{2\text{Re}[\tilde{C}_1\tilde{C}_2^*]}{|\tilde{C}_1|^2 + |\tilde{C}_2|^2\beta^2} \frac{((1 + \beta)^3 - 12(1 + 2\beta)(1 + \beta)x_\mu^2 + 16(1 + 3\beta)x_\mu^3)}{6(1 + \beta)^3} \left. \right\} \\
&\quad \times \theta[x_\mu - \frac{1 - \beta}{2}] \theta[\frac{1 + \beta}{2} - x_\mu] \left. \right].
\end{aligned} \tag{21}$$

Here, we put tildes on C_1 and C_2 . Integrating Γ and $d\Gamma/dx_\mu$ over the time, and summing them over B^0 decays and \bar{B}^0 decays, the energy distribution is represented by Eq. (21) replacing $|\tilde{C}_1|^2$, $|\tilde{C}_2|^2$, and $\text{Re}[\tilde{C}_1\tilde{C}_2^*]$ with $|C_1|^2$, $|C_2|^2$, and $(\text{Re}[C_1C_2^*] + \text{Re}[\bar{C}_1\bar{C}_2^*])/2$, respectively.

We depict this distribution and perform a Monte Carlo simulation (MC) to estimate the error of $(\text{Re}[C_1C_2^*] + \text{Re}[\bar{C}_1\bar{C}_2^*])/|2C_1C_2|$ in Figs. 2-4.

Fig. 2 represents the $|C_1| = |C_2| = 1$ case. Similarly, Fig. 3 and Fig. 4 represent the $\{|C_1|, |C_2|\} = \{1, 0.1\}$ and $\{|C_1|, |C_2|\} = \{0.1, 1\}$ cases, respectively. The interference effect emerges when $|C_1| \simeq |C_2|\beta$. We note here that in these figures, $\text{Re}[C_1C_2^*]$ independent point where $x_\mu \simeq 0.4$ is one of the solutions of identity, $(1 + \beta)^3 - 12(1 + 2\beta)(1 + \beta)x_\mu^2 + 16(1 + 3\beta)x_\mu^3 = 0$.

In Fig. 2, the MC is performed in a sample of 2000 events for $(\text{Re}[C_1C_2^*] + \text{Re}[\bar{C}_1\bar{C}_2^*])/|2C_1C_2| = 0$. The number of events are given as follows: The Super KEKB will make about 50 ab^{-1} integrated luminosity. The $e^+ + e^- \rightarrow \Upsilon(4S) \rightarrow B_d^0 \bar{B}_d^0$ cross section is about 10^{-33} cm^2 . The $B_d^0 \rightarrow \tau^+ \tau^-$ branching ratio is in Eq. (1). The $\tau^+ \rightarrow \mu^+ \nu_\mu \bar{\nu}_\tau$ branching ratio and the $\tau^+ \rightarrow e^+ \nu_e \bar{\nu}_\tau$ branching ratio are about 0.174 and 0.178. These are essentially the same events for the massless limit of daughter fermions. Therefore, about 2000 events will be available. The efficiency of this mode is in fact very low. However, we here just ignore it. The MC result is $(\text{Re}[C_1C_2^*] + \text{Re}[\bar{C}_1\bar{C}_2^*])/|2C_1C_2| = 0.11 \pm 0.10$.

In Figs. 3 and 4, the MC is performed in a sample of 20000 events for $(\text{Re}[C_1C_2^*] + \text{Re}[\bar{C}_1\bar{C}_2^*])/|2C_1C_2| = 0$. The MC results in $(\text{Re}[C_1C_2^*] + \text{Re}[\bar{C}_1\bar{C}_2^*])/|2C_1C_2|$ are -0.05 ± 0.21 and 0.17 ± 0.12 , respectively.

In the SM, $|C_1| \gg |C_2|$ [2]. Then, the coefficient $2\text{Re}[\tilde{C}_1\tilde{C}_2^*]/(|\tilde{C}_1|^2 + \beta|\tilde{C}_2|^2)$ is nearly zero. This situation is also realized if we set $\text{Re}[C_1C_2^*] =$

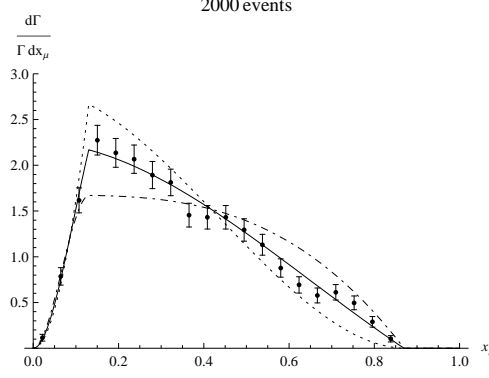


Figure 2: The μ energy distribution of $B^0 \rightarrow \tau^+\tau^-$ and subsequently $\tau^+ \rightarrow \mu^+(e^+) + \nu_{\mu(e)} + \bar{\nu}_\tau$ or $\tau^- \rightarrow \mu^-(e^-) + \bar{\nu}_{\mu(e)} + \nu_\tau$ decay, and their CP conjugate. The horizontal axis is the normalized μ energy x_μ . The vertical axis is the time integrated differential decay width $d\Gamma/dx_\mu$ over the time integrated partial width Γ . We set $|C_1| = |C_2| = 1$. The solid line, dashed line, and dot-dashed line represent $(\text{Re}[C_1 C_2^*] + \text{Re}[\bar{C}_1 \bar{C}_2^*])/|2C_1 C_2| = \{0, 1, -1\}$ case, respectively. The MC result in a sample of 2000 events for $(\text{Re}[C_1 C_2^*] + \text{Re}[\bar{C}_1 \bar{C}_2^*])/|2C_1 C_2| = 0$ is $(\text{Re}[C_1 C_2^*] + \text{Re}[\bar{C}_1 \bar{C}_2^*])/|2C_1 C_2| = 0.11 \pm 0.10$.

$\text{Re}[\bar{C}_1 \bar{C}_2^*] = 0$. Therefore, the shape of distribution is the same as $(\text{Re}[C_1 C_2^*] + \text{Re}[\bar{C}_1 \bar{C}_2^*])/|2C_1 C_2| = 0$ case.

$B \rightarrow \tau^+\tau^-$ energy distribution is very interesting since we can investigate the current structure of new physics.

For instance, Ref. [10] expresses the Higgs induced operators for the transition $b \rightarrow s\mu^+\mu^-$. It is easy to transform them for the transition $b \rightarrow d\tau^+\tau^-$. Completely, it is realized by the deformations $m_\mu \rightarrow m_\tau$, $F_{23} \rightarrow F_{13}$, $F_{32} \rightarrow F_{31}^*$, $\mu \rightarrow \tau$, and $s \rightarrow d$. After that, the coefficients C_1 and C_2 in this paper are given by

$$\begin{aligned} C_1 &= -\frac{1}{2G_F} \frac{m_\tau}{2v \cos \beta} \frac{\sin \beta}{M_A^2} (F_{13} + F_{31}^*) \\ C_2 &= -\frac{1}{2G_F} \frac{m_\tau}{2v \cos \beta} \left(\frac{\sin(\alpha - \beta) \cos \alpha}{M_H^2} - \frac{\cos(\alpha - \beta) \sin \alpha}{M_h^2} \right) (F_{13} - F_{31}^*). \end{aligned} \quad (22)$$

In Eq. (22), v , β , α , M_H , M_h , M_A , F_{13} , and F_{31} are vacuum expectation value, Higgs mixing angles, heavier neutral Higgs mass, lighter neutral Higgs mass, CP odd Higgs mass, and $b-d$ coupling constants, respectively, which are defined in Ref. [10]. This contribution can compete with or even dominate the SM one. Especially, in $M_A \rightarrow \infty$ limit, C_1 contains only the SM effect and C_2 contains only the 2HDM contribution.

On the other hand, the supersymmetric SM (SUSY) models without R-parity

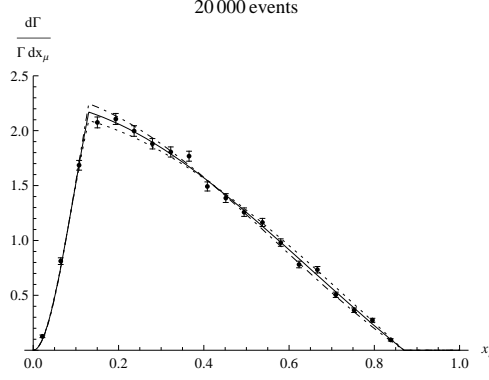


Figure 3: The absolute values of coefficients are $|C_1| = 1$ and $|C_2| = 0.1$. The number of event is 20000. Others are the same as Fig. 2. The MC result is $(Re[C_1 C_2^*] + Re[\bar{C}_1 \bar{C}_2^*]) / |2C_1 C_2| = -0.05 \pm 0.21$.

[11] suggest the coefficients

$$C_1 = -\frac{\lambda_{k33}^* \lambda'_{k3q} + \lambda_{k33} \lambda'^*_{kq3}}{4G_F m_{\tilde{l}_k}^2} \Big|_{(k \neq 3)} - \frac{2m_\tau}{m_B} \left\{ \frac{\lambda_{3k3}^* \lambda'_{3kq}}{8G_F m_{\tilde{q}_k}^2} + [C_A^q]_{\text{SM}} \right\} \quad (23)$$

$$C_2 = \frac{\lambda_{k33} \lambda'^*_{kq3} - \lambda_{k33}^* \lambda'_{k3q}}{4G_F m_{\tilde{l}_k}^2} \Big|_{(k \neq 3)},$$

where λ_{ijk} and λ'_{ijk} are the coefficients of $\hat{L}_i \hat{L}_j \hat{l}_k^c$ and $\hat{L}_i \hat{Q}_j \hat{d}_k^c$ type couplings, respectively, where \hat{L} , \hat{l}^c , \hat{Q} , and \hat{d}^c are the lepton doublet, lepton singlet, quark doublet, down-type quark singlet superfields, respectively; $m_{\tilde{l}_i}$ and $m_{\tilde{q}_i}$ are slepton and squark masses, respectively.

Moreover, leptquark models [12], the topcolor-assisted technicolor model [13], and the Babu-Kolda model [14] also deform the SM energy distribution, while the energy distribution in the multiscale walking technicolor model [15] is the same as the SM one. Considering the ratio $Br(B \rightarrow \tau\tau)/Br(B \rightarrow \mu\mu)$, SUSY models without R-parity [11], leptquark models [12], and the topcolor-assisted technicolor model [13] predictions differ from the SM one, while the Ref. [10], the Babu-Kolda model [14], and the multiscale walking technicolor model [15] predict the same value as the SM one. These characteristic features of models are available to distinguish them.

All of these models predict that the $Br(B \rightarrow \tau\tau)$ may become larger than the SM one.

2.2 Example 2 - τ^+ Decays into $\pi^+ \bar{\nu}_\tau$

We show here another example, in which B^0 decays into $\tau^+ \tau^-$ and subsequently $\tau^+ \rightarrow \pi^+ + \bar{\nu}_\tau$. In this case, we can set $G_1^a(y_a) = \delta(1 - y_\pi)/y_\pi^2$, $G_2^a(y_a) =$

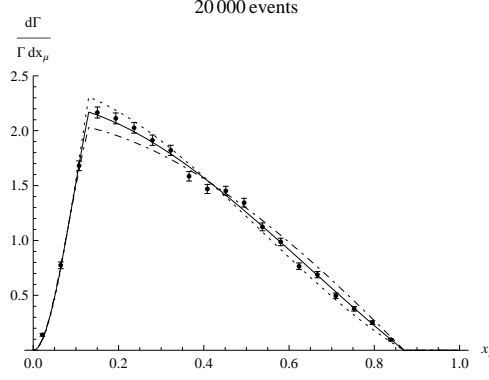


Figure 4: The absolute values of coefficients are $|C_1| = 0.1$ and $|C_2| = 1$. The number of event is 20000. Others are the same as Fig. 2. The MC result is $(Re[C_1 C_2^*] + Re[\tilde{C}_1 \tilde{C}_2^*]) / |2C_1 C_2| = 0.17 \pm 0.12$.

$-\delta(1 - y_\pi)/y_\pi$, $\lambda_a = 1$, and $\beta_a = \beta_b = \sqrt{1 - 4m_\tau^2/m_B^2} \equiv \beta$. Hence, the energy distribution is

$$\frac{1}{\Gamma} \frac{d\Gamma}{dx_\pi} = \frac{1}{\beta} \left\{ 1 - \frac{2Re[\tilde{C}_1 \tilde{C}_2^*]}{|\tilde{C}_1|^2 + |\tilde{C}_2|^2 \beta^2} (1 - 2x_\pi) \right\} \theta \left[x_\pi - \frac{1 - \beta}{2} \right] \theta \left[\frac{1 + \beta}{2} - x_\pi \right]. \quad (24)$$

In Figs. 5-7, we depict the time integrated distributions and the MC results for $(Re[C_1 C_2^*] + Re[\tilde{C}_1 \tilde{C}_2^*]) / |2C_1 C_2| = 0$ as the previous example. Fig. 5 represents the $|C_1| = |C_2| = 1$ case. Similarly, Fig. 6 and Fig. 7 represent the $\{|C_1|, |C_2|\} = \{1, 0.1\}$ and $\{|C_1|, |C_2|\} = \{0.1, 1\}$ cases, respectively. This mode is more suitable to understand the $B^0 \rightarrow \tau^+ \tau^-$ current structure than preceding one, since two-body decay does not dilute the polarization unlike the previous case, even though the $\tau^+ \rightarrow \pi^+ + \bar{\nu}_\tau$ branching ratio is about 0.11, which is smaller than the previous case.

The results of MC are as follows:

$$\begin{aligned} & \frac{Re[C_1 C_2^*] + Re[\tilde{C}_1 \tilde{C}_2^*]}{2|C_1 C_2|} \\ &= \begin{cases} -0.11 \pm 0.07 & \text{for } |C_1| = |C_2| = 1, & 600 \text{ events} \\ -0.21 \pm 0.15 & \text{for } |C_1| = 1, |C_2| = 0.1, & 6000 \text{ events} \\ -0.036 \pm 0.085 & \text{for } |C_1| = 0.1, |C_2| = 1, & 6000 \text{ events} \end{cases} \quad (25) \end{aligned}$$

3 Opening Angle Distribution

Here, we consider the opening angle Θ between particles a and b in B rest frame. The prescription is similar as Section 2, however, this time we multiply

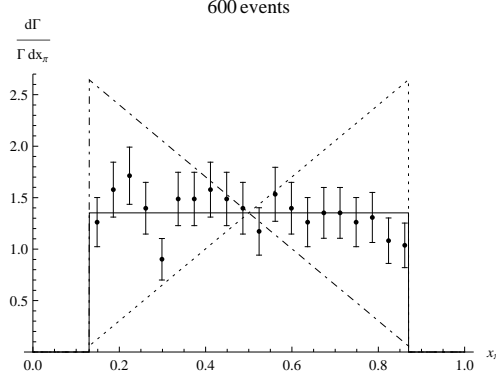


Figure 5: The π^+ energy distribution of $B^0 \rightarrow \tau^+\tau^-$ and subsequently $\tau^+ \rightarrow \pi^+ + \bar{\nu}_\tau$ or $\tau^- \rightarrow \pi^- + \nu_\tau$ decay, and their CP conjugate. The horizontal axis is the normalized π^+ energy x_π . The vertical axis is the time integrated differential decay width $d\Gamma/dx_\pi$ over the time integrated partial width Γ . We set $|C_1| = |C_2| = 1$. The number of events to perform MC for $(Re[C_1C_2^*] + Re[\bar{C}_1\bar{C}_2^*])/|2C_1C_2| = 0$ is 600. The solid line, dashed line, and dot-dashed line represent $(Re[C_1C_2^*] + Re[\bar{C}_1\bar{C}_2^*])/|2C_1C_2| = \{0, 1, -1\}$ case, respectively. $(Re[C_1C_2^*] + Re[\bar{C}_1\bar{C}_2^*])/|2C_1C_2| = -0.11 \pm 0.07$.

the different delta function

$$\delta\left[\cos\Theta - \frac{\sin\theta_a \sin\theta_b \cos\phi - \gamma_a\gamma_b(\beta_a + \cos\theta_a)(\beta_b - \cos\theta_b)}{(1 + \beta_a \cos\theta_a)(1 - \beta_b \cos\theta_b)\gamma_a\gamma_b}\right]. \quad (26)$$

Then, the result is

$$\begin{aligned} & \frac{1}{\Gamma} \frac{d\Gamma}{d\cos\Theta} \\ &= \frac{1}{4\pi} \int_{-1}^1 d\cos\theta_a \int_{B_{min}(\Theta, \theta_a)}^{B_{Max}(\Theta, \theta_a)} d\cos\theta_b \\ & \times \frac{(1 + \beta_a \cos\theta_a)(1 - \beta_b \cos\theta_b)\gamma_a\gamma_b}{\sqrt{\sin^2\theta_a \sin^2\theta_b - \gamma_a^2\gamma_b^2\{(1 + \beta_a \cos\theta_a)(1 - \beta_b \cos\theta_b)\cos\Theta + (\beta_a + \cos\theta_a)(\beta_b - \cos\theta_b)\}^2}} \\ & \times \left\{ 1 + \frac{D_4}{D_1} \left(\frac{m_b}{m_a} \cos\theta_a \langle G_2^a(y_a) \rangle + \frac{m_a}{m_b} \cos\theta_b \langle G_2^b(y_b) \rangle \right) \right. \\ & \quad - \left[\frac{D_2}{D_1} \gamma_a\gamma_b \{ (1 + \beta_a \cos\theta_a)(1 - \beta_b \cos\theta_b) \cos\Theta + (\beta_a + \cos\theta_a)(\beta_b - \cos\theta_b) \} \right. \\ & \quad \left. \left. - \cos\theta_a \cos\theta_b \right] \langle G_2^a(y_a) \rangle \langle G_2^b(y_b) \rangle \right\}, \end{aligned} \quad (27)$$

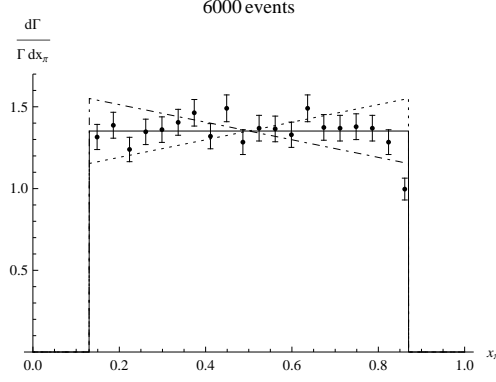


Figure 6: The absolute values of coefficients are $|C_1| = 1$ and $|C_2| = 0.1$. The number of event is 6000. Others are the same as Fig. 5. $(Re[C_1 C_2^*] + Re[\bar{C}_1 \bar{C}_2^*])/|2C_1 C_2| = -0.21 \pm 0.15$.

where we set

$$\begin{aligned} \int dy_a \frac{y_a^2}{\lambda_a} G_2^a(y_a) &\equiv \langle G_2^a(y_a) \rangle, \\ \int dy_b \frac{y_b^2}{\lambda_b} G_2^b(y_b) &\equiv \langle G_2^b(y_b) \rangle, \end{aligned} \quad (28)$$

$$\begin{aligned} &B_{Max,min}(\Theta, \theta_a) \\ &= \frac{\gamma_a^2 \gamma_b^2 \{(1 + \beta_a \cos \theta_a) \beta_b \cos \Theta + (\beta_a + \cos \theta_a)\} \{(1 + \beta_a \cos \theta_a) \cos \Theta + (\beta_a + \cos \theta_a) \beta_b\}}{\gamma_a^2 \gamma_b^2 \{(1 + \beta_a \cos \theta_a) \beta_b \cos \Theta + (\beta_a + \cos \theta_a)\}^2 + \sin^2 \theta_a} \\ &\pm \frac{\sin \theta_a \sqrt{\sin^2 \theta_a + \gamma_a^2 \{(\beta_a + \cos \theta_a)^2 - (1 + \beta_a \cos \theta_a)^2 \cos^2 \Theta\}}}{\gamma_a^2 \gamma_b^2 \{(1 + \beta_a \cos \theta_a) \beta_b \cos \Theta + (\beta_a + \cos \theta_a)\}^2 + \sin^2 \theta_a}. \end{aligned} \quad (29)$$

This expression suggests that the opening angle distribution determines $|C_1|$ and $|C_2|$, separately, via the coefficients D_2 .

If $f_a = f_b$, and the decay modes of \bar{f}_a and f_b are the same, for example, $B^0 \rightarrow \tau^+ \tau^- \rightarrow \pi^+ \pi^- \bar{\nu}_\tau \nu_\tau$ mode, the second term in Eq. (27) which has the coefficient D_4/D_1 will vanish because this term is antisymmetric about the $\cos \theta_a + \cos \theta_b = 0$ line, on the other hand, the domain of integration is symmetric.

3.1 Example 3 - τ^\pm Decay into μ^\pm

We here show a simple example that B^0 decays into $\tau^+ \tau^-$, and subsequently, they decay into $\mu^+ + \mu^- + \nu_\mu + \bar{\nu}_\mu + \nu_\tau + \bar{\nu}_\tau$. In this case, we set $\langle G_2^a(y_a) \rangle =$

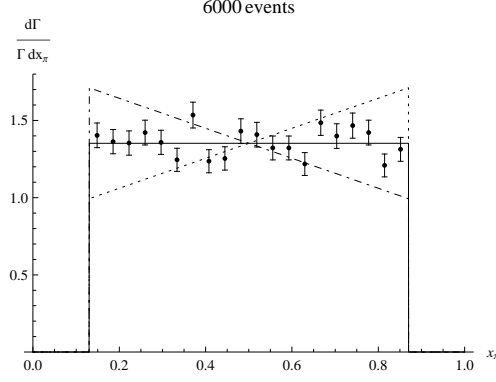


Figure 7: The absolute values of coefficients are $|C_1| = 0.1$ and $|C_2| = 1$. The number of event is 6000. Others are the same as Fig. 5. $(Re[C_1 C_2^*] + Re[\bar{C}_1 \bar{C}_2^*])/|2C_1 C_2| = -0.036 \pm 0.085$.

$\langle G_2^b(y_b) \rangle = 1/3$. The numerical result is depicted in Fig. 8. We perform the MC for $(|C_1|^2 - |C_2|^2 \beta^2)/(|C_1|^2 + |C_2|^2 \beta^2) = 0$ in a sample of 35000 events, which corresponds to the 100 times of 50 ab^{-1} . The result is $(|C_1|^2 - |C_2|^2 \beta^2)/(|C_1|^2 + |C_2|^2 \beta^2) = -0.15 \pm 0.18$.

In this figure, the increase near $\cos \Theta = -1$ is caused by the back-to-back Lorentz boost of \bar{f}_a and f_b along the z axis.

If new physics affects this mode substantially, we may detect the distribution. In that case, $B \rightarrow \tau^+ \tau^-$ opening angle distribution is useful to distinguish new physics models. In the SM, $|C_1| \gg |C_2|$ [2]. Then, the shape of distribution is the same as $(|C_1|^2 - |C_2|^2 \beta^2)/(|C_1|^2 + |C_2|^2 \beta^2) = +1$ case. However, many new physics models, for example, Refs. [10], [11], [12], [13], and [14], deform the shape of distribution near $\cos \Theta = -1$.

3.2 Example 4 - τ^\pm Decay into π^\pm

We show another example that B^0 decays into $\tau^+ \tau^-$, and subsequently, they decay into $\pi^+ + \pi^- + \nu_\tau + \bar{\nu}_\tau$. In this case, we set $\langle G_2^a(y_a) \rangle = \langle G_2^b(y_b) \rangle = 1$. The numerical result is depicted in Fig. 9. We perform the MC for $(|C_1|^2 - |C_2|^2 \beta^2)/(|C_1|^2 + |C_2|^2 \beta^2) = 0$ in a sample of 40 events, which will given in the Super B-factory. The MC result is $(|C_1|^2 - |C_2|^2 \beta^2)/(|C_1|^2 + |C_2|^2 \beta^2) = 0.03 \pm 0.49$.

In this figure, the dashed line decreases near $\cos \Theta = -1$, on the other hand, the dot-dashed line increases there. The reason is as follows: In this case, the second term in Eq. (27) is vanished, and we can set $\beta_a = \beta_b \equiv \beta$. Therefore, for $\cos \Theta = -1$, Eq. (27) is proportional to

$$\left\{ \left(1 + \frac{D_2}{D_1} \right) (1 + \cos \theta_a \cos \theta_b) \right\}. \quad (30)$$

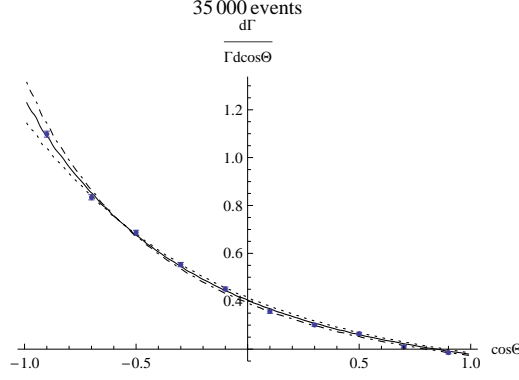


Figure 8: The opening angle distribution between μ^+ and μ^- in $B^0 \rightarrow \tau^+ \tau^- \rightarrow \mu^+ + \mu^- + \nu_\tau \bar{\nu}_\tau \nu_\mu \bar{\nu}_\mu$ decay. The horizontal axis is $\cos \Theta$, and the vertical axis is time integrated $d\Gamma/d\cos\Theta$ over time integrated Γ . The solid line, dashed line, and dot-dashed line represent $(|C_1|^2 - |C_2|^2\beta^2)/(|C_1|^2 + |C_2|^2\beta^2) = \{0, 1, -1\}$ cases, respectively. The MC result for $(|C_1|^2 - |C_2|^2\beta^2)/(|C_1|^2 + |C_2|^2\beta^2) = 0$ is $(|C_1|^2 - |C_2|^2\beta^2)/(|C_1|^2 + |C_2|^2\beta^2) = -0.15 \pm 0.18$ in a sample of 35000 events.

The factor $1 + D_2/D_1$ becomes zero when C_2 is zero, and it becomes maximum when C_1 is zero.

4 Azimuthal Angle Asymmetry

Generally, the trajectories of a and b draw the skew lines since \bar{f}_a and f_b have the finite lifetimes. If the vertex detector of B-factory could detect the decay points of \bar{f}_a and f_b , we were able to determine ϕ dependence of $d\Gamma$, and then $Im[C_1 C_2^*]$. However, some of \bar{f}_a and f_b decay into one-prong modes, the polarization effect is diluted in the many body decays, and/or the vertex detector does not have sufficient resolution to detect the decay points accurately. Thus, we consider another method to determine $Im[C_1 C_2^*]$.

Since ϕ is the azimuthal angle between a and b as depicted in Fig. 1, the Lorentz boost along z direction has no effect on this angle. Thus, the delta function is unnecessary unlike the Sections 2 and 3.

The trajectories of a and b in B rest frame are written as

$$\begin{aligned} \mathbf{q}_a(t_a) &= \{\sin\theta_a t_a, 0, (\beta_a \gamma_a + \gamma_a \cos\theta_a)t_a + d_z\} \\ \mathbf{q}_b(t_b) &= \{\sin\theta_b \cos\phi t_b, \sin\theta_b \sin\phi t_b, (-\beta_b \gamma_b + \gamma_b \cos\theta_b)t_b\}, \end{aligned} \quad (31)$$

where t_a and t_b are the parameters.

The vector product of $\mathbf{q}_a(t_a)$ and $\mathbf{q}_b(t_b)$ for $d_z \rightarrow 0$, $t_a > 0$, and $t_b > 0$ takes

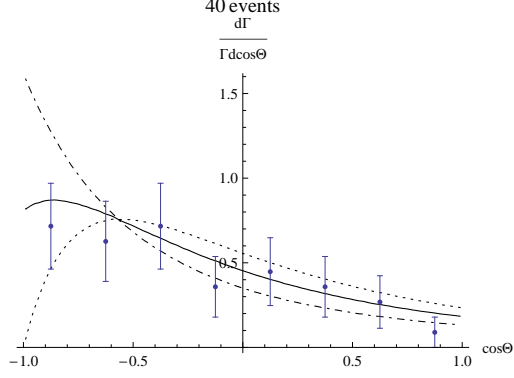


Figure 9: The opening angle distribution between π^+ and π^- in $B^0 \rightarrow \tau^+ \tau^- \rightarrow \pi^+ + \pi^- + \nu_\tau \bar{\nu}_\tau$ decay. The horizontal axis is $\cos \Theta$, and the vertical axis is $d\Gamma/(\Gamma d \cos \Theta)$. The solid line, dashed line, and dot-dashed line represent $(|C_1|^2 - |C_2|^2 \beta^2)/(|C_1|^2 + |C_2|^2 \beta^2) = \{0, 1, -1\}$ cases, respectively. The MC result for $(|C_1|^2 - |C_2|^2 \beta^2)/(|C_1|^2 + |C_2|^2 \beta^2) = 0$ is $(|C_1|^2 - |C_2|^2 \beta^2)/(|C_1|^2 + |C_2|^2 \beta^2) = 0.03 \pm 0.49$ in a sample of 40 events.

the form

$$\begin{aligned} & \mathbf{q}_a(t_a) \times \mathbf{q}_b(t_b) \Big|_{d_z \rightarrow 0, t_a > 0, t_b > 0} \\ &= t_a t_b \begin{pmatrix} -\gamma_a(\beta_a + \cos \theta_a) \sin \theta_b \sin \phi \\ \gamma_a(\beta_a + \cos \theta_a) \sin \theta_b \cos \phi - \sin \theta_a \gamma_b(-\beta_b + \cos \theta_b) \\ \sin \theta_a \sin \theta_b \sin \phi \end{pmatrix}. \end{aligned} \quad (32)$$

Meanwhile, the difference between $\mathbf{q}_a(t'_a)$ and $\mathbf{q}_b(t'_b)$ is

$$\mathbf{q}_a(t'_a) - \mathbf{q}_b(t'_b) = \begin{pmatrix} \sin \theta_a t'_a - \sin \theta_b \cos \phi t'_b \\ -\sin \theta_b \sin \phi t'_b \\ \gamma_a(\beta_a + \cos \theta_a) t'_a + d_z - \gamma_b(-\beta_b + \cos \theta_b) t'_b \end{pmatrix}, \quad (33)$$

where t'_a and t'_b are the parameters of $\mathbf{q}_a(t'_a)$ and $\mathbf{q}_b(t'_b)$. t'_a and t'_b take arbitrary values. The scalar product between Eq. (32) and Eq. (33) is given by

$$\mathbf{q}_a(t_a) \times \mathbf{q}_b(t_b) \Big|_{d_z \rightarrow 0, t_a > 0, t_b > 0} \cdot \{\mathbf{q}_a(t'_a) - \mathbf{q}_b(t'_b)\} = t_a t_b d_z \sin \theta_a \sin \theta_b \sin \phi. \quad (34)$$

This quantity becomes plus as $0 < \phi < \pi$ and minus as $\pi < \phi < 2\pi$. The sign of $\sin \phi$ is determined event-by-event (See Fig. 10). Then, the azimuthal angle asymmetry

$$\int_0^\pi d\phi \frac{1}{\Gamma} \frac{d\Gamma}{d\phi} - \int_\pi^{2\pi} d\phi \frac{1}{\Gamma} \frac{d\Gamma}{d\phi} = -\frac{\pi}{8} \frac{D_5}{D_1} \langle G_2^a(y_a) \rangle \langle G_2^b(y_b) \rangle \quad (35)$$

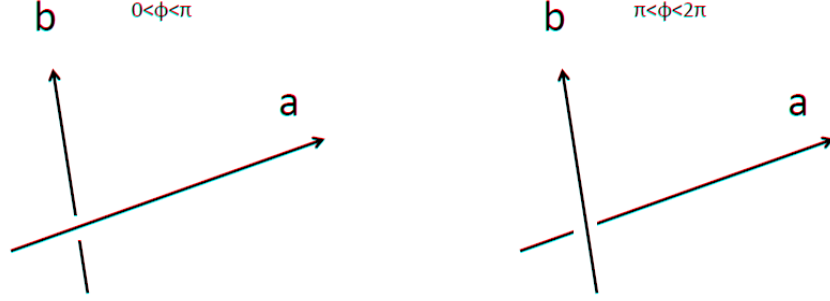


Figure 10: Interpolating the trajectories, the skew lines take two types of alignments. The left one corresponds to $0 < \phi < \pi$. The right one corresponds to $\pi < \phi < 2\pi$.

gives us the coefficient D_5 , which is proportional to $Im[C_1 C_2^*]$.

We perform the MC for $B^0 \rightarrow \tau^+ + \tau^-$ and then $\tau^+ \rightarrow \pi^+ \bar{\nu}_\tau$ and $\tau^- \rightarrow \pi^- \nu_\tau$. We set $(Im[C_1 C_2^*] + Im[\bar{C}_1 \bar{C}_2^*])/|2C_1 C_2| = 0$ and summarize the results in table 1.

Table 1: The MC for $(Im[C_1 C_2^*] + Im[\bar{C}_1 \bar{C}_2^*])/|2C_1 C_2| = 0$ and some conditions

$ C_1 , C_2 $	number of events	$\frac{Im[C_1 C_2^*] + Im[\bar{C}_1 \bar{C}_2^*]}{2 C_1 C_2 }$ and error
$ C_1 = C_2 = 1$	40	-0.40 ± 0.64
$ C_1 = C_2 = 1$	400	-0.053 ± 0.19
$ C_1 = 1, C_2 = 0.1$	4000	0.078 ± 0.39

5 Only One of Two Fermions is Unstable

If f_b is a stable particle, for example, $B_d^0 \rightarrow \bar{\Lambda}_c^- p$, $B_u^+ \rightarrow \bar{\Sigma}_c(2455)^0 p$, $B^+ \rightarrow \tau^+ \nu_\tau$, $B^0 \rightarrow \tau^+ e^-$, and $B^0 \rightarrow \tau^+ \mu^-$, the general formula (15) is modified to form

$$\frac{d\Gamma}{dy_a d\Omega_a} = Br_a \frac{y_a^2}{4\pi\lambda_a} \frac{f_B^2 G_F^2}{2\pi} |\mathbf{p}| \left\{ D_1 G_1^a(y_a) + D_4 \frac{m_b}{m_a} \cos\theta_a G_2^a(y_a) \right\}. \quad (36)$$

Then, by the similar calculations, the partial decay width is

$$\Gamma = Br_a \frac{f_B^2 G_F^2}{2\pi} |\mathbf{p}| D_1, \quad (37)$$

the a energy distribution is

$$\frac{1}{\Gamma} \frac{d\Gamma}{dx_a} = \int dy_a \frac{1}{\beta_a \lambda_a} \left\{ y_a G_1^a(y_a) + \frac{D_4}{D_1} \frac{m_b}{m_a \beta_a} (2x_a - y_a) G_2^a(y_a) \right\}, \quad (38)$$

where $\int dy_a$ means the same as before, and the distribution of the opening angle Θ' between f_b and a is

$$\frac{1}{\Gamma} \frac{d\Gamma}{d\cos\Theta'} = \frac{1}{2} \frac{1 - \beta_a^2}{(1 + \beta_a \cos\Theta')^2} \left\{ 1 - \frac{D_4}{D_1} \frac{m_b}{m_a} \frac{\cos\Theta' + \beta_a}{1 + \beta_a \cos\Theta'} \langle G_2^a(y_a) \rangle \right\}, \quad (39)$$

where

$$\cos\Theta' = -\frac{\beta_a + \cos\theta_a}{1 + \beta_a \cos\theta_a}. \quad (40)$$

Both of these two distributions give D_4 . These are used for a cross-check. However, we cannot pull out D_2 and D_5 . The energy distribution is useful even if f_b is a missing fermion except for neutrinos. If f_b is a neutrino, $m_b \rightarrow 0$ and the second terms in both of Eqs. (38) and (39) are vanish, and then we cannot determine D_4 .

5.1 Example 5 - $B^0 \rightarrow \tau^+ \mu^-, \tau^+ \rightarrow \pi^+ \bar{\nu}_\tau$

We consider the lepton flavor violating $B^0 \rightarrow \tau^+ \mu^-$ decay, and subsequently τ^+ decays into $\pi^+ \bar{\nu}_\tau$. In this case, we can set $G_1^a(y_a) = \delta(1 - y)/y^2$, $G_2^a(y_a) = -\delta(1 - y)/y$, $\lambda_a = 1$, and $\langle G_2^a(y_a) \rangle = 1$.

The a energy distribution is

$$\frac{1}{\Gamma} \frac{d\Gamma}{dx_a} = \frac{1}{\beta_\tau} \left\{ 1 - \frac{D_4}{D_1} \frac{m_\mu}{m_\tau \beta_\tau} (2x_\tau - 1) \right\} \theta \left[x_\tau - \frac{1 - \beta_\tau}{2} \right] \theta \left[\frac{1 + \beta_\tau}{2} - x_\tau \right]. \quad (41)$$

On the other hand, the opening angle distribution takes the form

$$\frac{1}{\Gamma} \frac{d\Gamma}{d\cos\Theta'} = \frac{1}{2} \frac{1 - \beta_\tau^2}{(1 + \beta_\tau \cos\Theta')^2} \left\{ 1 - \frac{D_4}{D_1} \frac{m_\mu}{m_\tau} \frac{\cos\Theta' + \beta_\tau}{1 + \beta_\tau \cos\Theta'} \right\}. \quad (42)$$

These distributions and the MC for $(Re[C_1 C_2^*] + Re[\bar{C}_1 \bar{C}_2^*])/|2C_1 C_2| = 0$ in a sample of 10000 events are depicted in Figs. 11 and 12. The results are $(Re[C_1 C_2^*] + Re[\bar{C}_1 \bar{C}_2^*])/|2C_1 C_2| = 0.27 \pm 0.29$ and -0.03 ± 0.30 , respectively. They have almost the same errors.

The SUSY models without R-parity [16] suggest the coefficients

$$\begin{aligned} C_1 &= -\frac{1}{4G_F} \left\{ \frac{m_B}{m_b} (C_{2S}^+ + C_{1S}^+) - \frac{m_\tau}{m_B} C_V^+ \right\} \\ C_2 &= -\frac{1}{4G_F} \left\{ \frac{m_B}{m_b} (C_{2S}^+ - C_{1S}^+) - \frac{m_\tau}{m_B} C_V^+ \right\}, \end{aligned} \quad (43)$$

where C_{1S}^+ , C_{2S}^+ , and C_V^+ are defined in Ref. [16] as

$$C_{1S}^+ = \sum_{i \neq 3} \frac{\lambda'_{i3q} \lambda_{i32}^*}{m_{\tilde{\nu}_i}^2}, \quad C_{2S}^+ = \sum_{i \neq 2} \frac{\lambda'_{iq3} \lambda_{i23}^*}{m_{\tilde{\nu}_i}^2}, \quad C_V^+ = \sum_i \frac{\lambda'_{2iq} \lambda_{3i3}^*}{2m_{\tilde{q}_i}^2}, \quad (44)$$

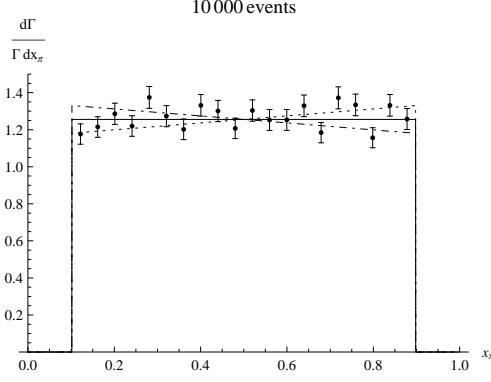


Figure 11: The energy distribution of π^+ in $B^0 \rightarrow \tau^+ \mu^-$, $\tau^+ \rightarrow \pi^+ \bar{\nu}_\tau$ for $|C_1| = |C_2| = 1$. The solid line, the dashed line, and the dot-dashed line represent $(Re[C_1 C_2^*] + Re[\bar{C}_1 \bar{C}_2^*])/|2C_1 C_2| = \{0, 1, -1\}$, respectively. The MC is performed for $(Re[C_1 C_2^*] + Re[\bar{C}_1 \bar{C}_2^*])/|2C_1 C_2| = 0$ in a sample of 10000 events to result in $(Re[C_1 C_2^*] + Re[\bar{C}_1 \bar{C}_2^*])/|2C_1 C_2| = 0.27 \pm 0.29$.

where $m_{\tilde{\nu}_i}$ is squark mass. In this model, the branching ratio can become about 10^{-5} , which is the same order as the experimental upper bound, and it has a relation, $Br(B \rightarrow \mu\mu) \lesssim Br(B \rightarrow \tau\mu) \lesssim Br(B \rightarrow \tau\tau)$. Moreover, since this mode has only one neutrino, the efficiency is much higher than that of $B \rightarrow \tau\tau$ mode.

6 Example 6 - $B_u^+ \rightarrow \Xi_c^0 \Lambda_c^+$ and $\bar{B}^0 \rightarrow \Lambda_c^+ \bar{p}$ Decay

Now we show two baryon modes for examples. The first one is $B_u^+ \rightarrow \Xi_c^0 \Lambda_c^+$ decay. According to Ref. [5], in the SM, we have the relation for B^+

$$\frac{C_1}{C_2} = -\frac{m_{\Xi_c}^2 - (m_B - m_{\Lambda_c})^2}{m_B^2 - (m_{\Xi_c} - m_{\Lambda_c})^2} = 0.10, \quad (45)$$

where m_{Ξ_c} and m_{Λ_c} are Ξ_c^0 and Λ_c^+ masses, respectively. Then, we predict

$$\frac{D_2}{D_1} = 0.89, \quad \frac{D_4}{D_1} = -0.45, \quad \frac{D_5}{D_1} = 0. \quad (46)$$

This prediction is available for the test of Ref. [5].

The next one is $\bar{B}^0 \rightarrow \Lambda_c^+ \bar{p}$ decay. According to the Ref. [17], which uses the factorization,

$$\frac{|C_2|}{|C_1|} = 0.34. \quad (47)$$

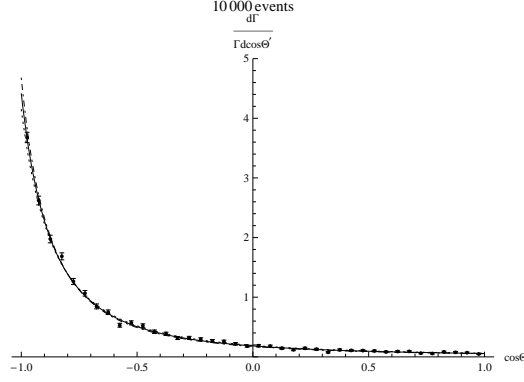


Figure 12: The distribution of opening angle between μ^- and π^+ in the same process as Fig. 11. The solid line, the dashed line, and the dot-dashed line represent $(Re[C_1 C_2^*] + Re[\bar{C}_1 \bar{C}_2^*])/|2C_1 C_2| = \{0, 1, -1\}$, respectively. The MC is performed for $(Re[C_1 C_2^*] + Re[\bar{C}_1 \bar{C}_2^*])/|2C_1 C_2| = 0$ in a sample of 10000 events to result in $(Re[C_1 C_2^*] + Re[\bar{C}_1 \bar{C}_2^*])/|2C_1 C_2| = -0.03 \pm 0.30$.

Then, if $C_1 C_2^*$ has no relative phase (or $Re[C_1 C_2^*] = |C_1 C_2|$),

$$\frac{D_4}{D_1} = -0.52. \quad (48)$$

On the other hand, according to Ref. [18], which uses the pole model,

$$\frac{|C_2|}{|C_1|} = 0.77 \quad (49)$$

in $\bar{B}^0 \rightarrow \Lambda_c^+ \bar{p}$ decay. Therefore, if $C_1 C_2^*$ has no relative phase (or $Re[C_1 C_2^*] = |C_1 C_2|$),

$$\frac{D_4}{D_1} = -0.90. \quad (50)$$

These two models suggest different branching ratio and $|C_2/C_1|$. The different branching ratio may be corrected by the non-perturbative QCD effect. However, $|C_2/C_1|$ eminently represents the feature of each model. Hence, we can test which model works better.

The QCD effect may pollute new physics effect. However, at least, one of these observables is measured to considerably differ from (46), or (48) and (50), we should take into account new physics. We point out that more observables are desirable for new physics discovery.

Theoretically, deriving the precise expressions of G_1 and G_2 is not easy. However, we are interested in $B \rightarrow \bar{f}_a f_b$ decays. We assume that there is no new physics contribution in the Ξ_c^0 and Λ_c^+ decays. So, it is not necessary for

us to know the expressions of G_1 and G_2 theoretically if we can determine it from the experimental data. Actually, Refs. [4], [19], [20], and [21] suggest the Λ_c polarization, also Ref. [22] measures the Ξ_c^0 polarization. In this reference, Ξ_c^0 decays into $\Xi^-\pi^+$. The two body decay makes G_1 and G_2 trivially. Then, these decays are given by

$$\begin{aligned}\frac{dBr(\bar{\Xi}_c^0 \rightarrow \pi^- + p^+)}{d^3k_{\pi^-}} &= \frac{2Br_{\bar{\Xi}_c^0}}{\pi m_{\pi^-}^3} \left[\frac{\delta(1 - y_{\pi^-})}{y_{\pi^-}^2} - \alpha_{\Xi_c} \mathbf{s}^{\bar{\Xi}_c^0} \cdot \hat{\mathbf{k}}_{\pi^-} \frac{\delta(1 - y_{\pi^-})}{y_{\pi^-}} \right] \\ \frac{dBr(\Lambda_c^+ \rightarrow \pi^+ + \Lambda)}{d^3k_{\pi^+}} &= \frac{2Br_{\Lambda_c^+}}{\pi m_{\pi^+}^3} \left[\frac{\delta(1 - y_{\pi^+})}{y_{\pi^+}^2} + \alpha_{\Lambda_c} \mathbf{s}^{\Lambda_c^+} \cdot \hat{\mathbf{k}}_{\pi^+} \frac{\delta(1 - y_{\pi^+})}{y_{\pi^+}} \right],\end{aligned}\tag{51}$$

where $Br_{\bar{\Xi}_c^0} = Br(\bar{\Xi}_c^0 \rightarrow \pi^- + p^+)$ and $Br_{\Lambda_c^+} = Br(\Lambda_c^+ \rightarrow \pi^+ + \Lambda)$; m_{π^\pm} are the charged pion masses, y_{π^\pm} are normalized charged pion energies defined by the same manner as in Eq. (16); α_{Ξ_c} and α_{Λ_c} are the decay parameters; $\mathbf{s}^{\bar{\Xi}_c^0}$ and $\mathbf{s}^{\Lambda_c^+}$ are the polarization vectors of $\bar{\Xi}_c^0$ and Λ_c^+ , respectively; \mathbf{k}_{π^\pm} are the π^\pm momenta, respectively.

Fig. 13 explains the $B_u^+ \rightarrow \bar{\Xi}_c^0 + \Lambda_c^+$, $\Lambda_c^+ \rightarrow \Lambda + \pi^+$, and $\bar{\Xi}_c^0 \rightarrow p^+ + \pi^-$ decay Monte Carlo simulation with 320 and 16000 events. The horizontal region is determined by the π^+ energy distribution and the diagonal region is determined by the $\pi^+\pi^-$ opening angle distribution. The dot represents Eq. (46). The simulation is performed with this parameter set and the decay parameters, $\alpha_{\Xi_c} = -0.6$ and $\alpha_{\Lambda_c} = -0.91$. We have to consider that α_{Ξ_c} has a large ambiguity $\alpha_{\Xi_c} = -0.6 \pm 0.4$. So, we explain α_{Ξ_c} dependence in Figs. 14 and 15.

Fig. 16 represents the π^+ energy distribution of $\bar{B}^0 \rightarrow \Lambda_c^+ \bar{p}$ and $\Lambda_c^+ \rightarrow \Lambda + \pi^+$ decay chain. The lighter gray explains $|C_2|/|C_1| = 0.77$ case and the darker gray does $|C_2|/|C_1| = 0.34$ case. These distributions have breadth caused by the ambiguity in $\alpha_{\Lambda_c} = -0.91 \pm 0.15$. The results of Monte Carlo simulation with 200 and 10000 events are

$$\begin{aligned}\alpha_{\Lambda_c} \frac{D_4}{D_1} &= 0.72 \pm 0.27, \\ \alpha_{\Lambda_c} \frac{D_4}{D_1} &= 0.83 \pm 0.04,\end{aligned}\tag{52}$$

respectively.

7 Summary and Discussion

We studied the current structure of $B \rightarrow \bar{f}_a f_b$ decay modes using polarization effects. This can be applied to both of leptonic and baryonic decays, also, to the charged and neutral B mesons.

The a energy distribution gives $Re[C_1 C_2^*]$. If we consider no or small relative phase between C_1 and C_2^* , we can estimate the ratio of $|C_1|$ and $|C_2|$. The energy distribution of a and b gives no more information.

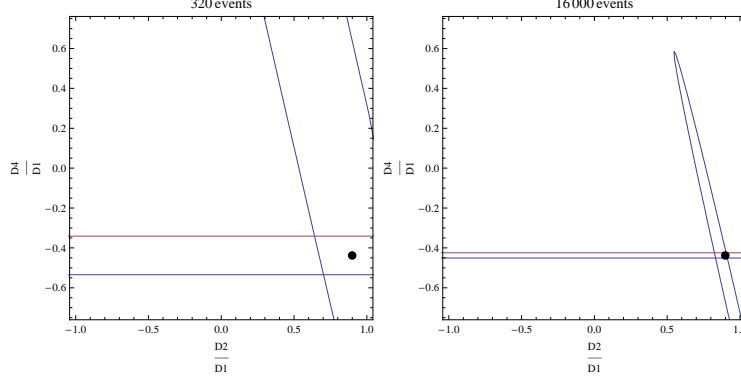


Figure 13: The allowed region determined by the energy distribution and opening angle distribution of $B_u^+ \rightarrow \bar{\Xi}_c^0 + \Lambda_c^+$, $\Lambda_c^+ \rightarrow \Lambda + \pi^+$, and $\bar{\Xi}_c^0 \rightarrow p^+ + \pi^-$ decay chain. The left and right figures are the results of MC simulation with 320 and 16000 events, respectively. In each figure, the dot means the SM prediction. The horizontal lines explain the allowed region which is determined by the energy distribution. The diagonal region is allowed by the opening angle distribution. $D_4/D_1 = -0.44 \pm 0.10$ for 320 events. $D_4/D_1 = -0.44 \pm 0.01$ for 16000 events.

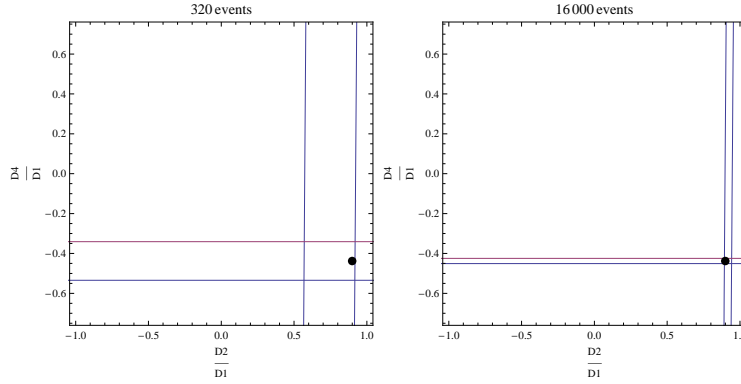


Figure 14: Same as Fig. 13 but, we here use $\alpha_{\Xi_c} = -0.6 - 0.4$. The diagonal region in Fig. 13 becomes narrower and more vertically.

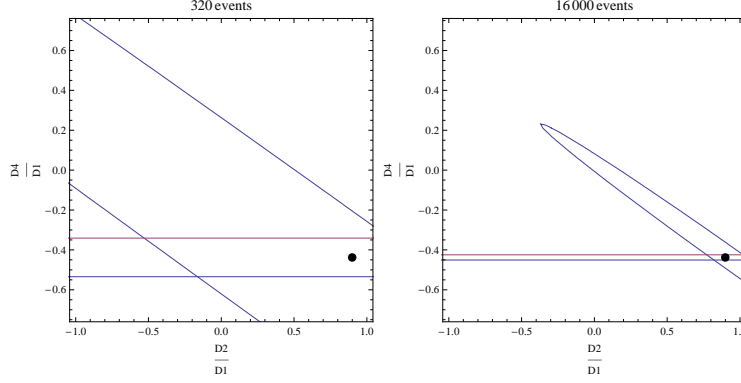


Figure 15: Same as Fig. 13 but, we here use $\alpha_{\Xi_c} = -0.6 + 0.4$. The diagonal region in Fig. 13 becomes wider and is inclined more horizontally.

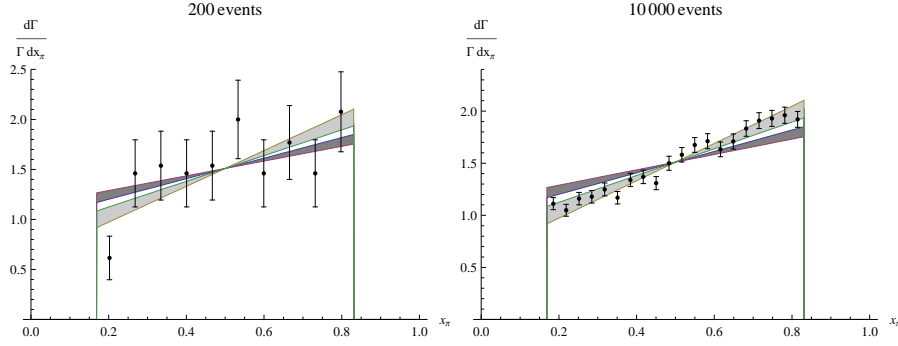


Figure 16: The π^+ energy distribution of $\bar{B}^0 \rightarrow \Lambda_c^+ \bar{p}$ and $\Lambda_c^+ \rightarrow \Lambda + \pi^+$ decay chain. The lighter gray explains $|C_2/C_1| = 0.77$ case and the darker gray does $|C_2/C_1| = 0.34$ case. These have breadth caused by the ambiguity in $\alpha_{\Lambda_c} = 0.91 \pm 0.15$. The dots with error bar are the result of MC simulation for $|C_2/C_1| = 0.77$ case with 200 (left figure) and 10000 (right figure) events. These suggest that $\alpha_{\Lambda_c} D_4/D_1 = 0.72 \pm 0.27$ (left figure) and $\alpha_{\Lambda_c} D_4/D_1 = 0.83 \pm 0.04$ (right figure).

The opening angle Θ distribution gives $|C_1|$ and $|C_2|$, separately. With the energy distribution, this gives us the relative phase between C_1 and C_2^* up to a binary ambiguity.

The azimuthal angle ϕ asymmetry gives $Im[C_1 C_2^*]$. We cannot detect the decay point in the one-prong events. Then, we cannot determine the ϕ distribution. However, we can determine that ϕ is larger or smaller than π . This is enough to give $Im[C_1 C_2^*]$.

If one of two fermions is stable particle, we cannot determine D_2 and D_5 . However, D_4 is determined by each of the $\cos \Theta'$ and the x_a distribution.

We predicted D_4/D_1 and D_2/D_1 of the baryon modes $B_u^+ \rightarrow \Xi_c^0 \Lambda_c^+$ and $\bar{B}^0 \rightarrow \Lambda_c^+ \bar{p}$. They are summarized in Figs. 13-16.

In the Examples 1-4, we derived the $B_d^0 \rightarrow \tau^+ \tau^-$ sample number ignoring the efficiency. Here, we try to consider it. According to Ref. [23], they conclude $Br(B_d^0 \rightarrow \tau^+ \tau^-) < 4.1 \times 10^{-3}$ using $(232 \pm 3) \times 10^6$ data sample, which corresponds to 210 fb^{-1} . Hence, we need 7.9×10^{12} ($7.2 \times 10^3 \text{ ab}^{-1}$) data sample to discover a $B_d^0 \rightarrow \tau^+ \tau^-$ event with the same efficiency as Ref. [23]. This efficiency can be improved, for example, by the semileptonic tagging method [24]. However, it is difficult to detect this mode in the SM case. If $B_d^0 \rightarrow \tau^+ \tau^-$ is detected, it must be induced by new physics. Then, our analysis is useful to determine its current structure.

In the neutral B decays, \tilde{C}_1 and \tilde{C}_2 are the functions of t as defined in Eq. (10). If we determine $|\tilde{C}_1|^2$, $|\tilde{C}_2|^2$, $Re[\tilde{C}_1 \tilde{C}_2^*]$, and $Im[\tilde{C}_1 \tilde{C}_2^*]$, respectively, then, using their t dependence, we can derive the time independent coefficients. The result is summarized as follows:

$$\begin{aligned}
|\tilde{C}_1|^2 &\Rightarrow |C_1|^2, \left| \frac{q}{p} \right|^2 |\bar{C}_1|^2, Re[C_1 \frac{q^*}{p^*} \bar{C}_1^*], Im[C_1 \frac{q^*}{p^*} \bar{C}_1^*] \\
|\tilde{C}_2|^2 &\Rightarrow |C_2|^2, \left| \frac{q}{p} \right|^2 |\bar{C}_2|^2, Re[C_2 \frac{q^*}{p^*} \bar{C}_2^*], Im[C_2 \frac{q^*}{p^*} \bar{C}_2^*] \\
Re[\tilde{C}_1 \tilde{C}_2^*] &\Rightarrow Re[C_1 C_2^*], \left| \frac{q}{p} \right|^2 Re[\bar{C}_1 \bar{C}_2^*], \\
Re[C_1 \frac{q^*}{p^*} \bar{C}_2^*] &+ Re[\frac{q}{p} \bar{C}_1 C_2^*], Im[C_1 \frac{q^*}{p^*} \bar{C}_2^*] - Im[\frac{q}{p} \bar{C}_1 C_2^*] \\
Im[\tilde{C}_1 \tilde{C}_2^*] &\Rightarrow Im[C_1 C_2^*], \left| \frac{q}{p} \right|^2 Im[\bar{C}_1 \bar{C}_2^*], \\
Re[C_1 \frac{q^*}{p^*} \bar{C}_2^*] &- Re[\frac{q}{p} \bar{C}_1 C_2^*], Im[C_1 \frac{q^*}{p^*} \bar{C}_2^*] + Im[\frac{q}{p} \bar{C}_1 C_2^*].
\end{aligned} \tag{53}$$

To determine these quantities, we need a huge number of statistics.

In Examples 1-5 (and $\bar{B}^0 \rightarrow \Lambda_c^+ \bar{p}$ in Example 6), we integrated over the time dependence, and took sum over B^0 (\bar{B}^0) decay events and their CP conjugate. However, if we take difference between the B^0 decay events and their CP

conjugate instead of sum, we obtain

$$\begin{aligned} & \frac{X_B}{1+X_B^2} \text{Im}\left[\frac{q}{p} C_1 \bar{C}_1^*\right], & \frac{X_B}{1+X_B^2} \text{Im}\left[\frac{q}{p} C_2 \bar{C}_2^*\right], \\ & \frac{1}{1+X_B^2} (\text{Re}[C_1 C_2^*] - \text{Re}[\bar{C}_1 \bar{C}_2^*]) + \frac{X_B}{1+X_B^2} (\text{Im}\left[\frac{p}{q} C_1 \bar{C}_2^*\right] - \text{Im}\left[\frac{p^*}{q^*} \bar{C}_1 C_2^*\right]), & (54) \\ & \frac{1}{1+X_B^2} (\text{Im}[C_1 C_2^*] - \text{Im}[\bar{C}_1 \bar{C}_2^*]) - \frac{X_B}{1+X_B^2} (\text{Re}\left[\frac{p}{q} C_1 \bar{C}_2^*\right] - \text{Re}\left[\frac{p^*}{q^*} \bar{C}_1 C_2^*\right]), \end{aligned}$$

where $X_B = \Delta m_B / \Gamma_B$. If we detect at least one of them, it means that CP is violated.

In the Examples 1-5, we showed some simple processes. We can determine the parameters more precisely by using not only these processes but also $\tau^+ \rightarrow \pi^+ \pi^0 \bar{\nu}_\tau$ and other processes.

In Section 5, we studied the case that only one of two fermions is unstable. $B \rightarrow \tau \mu$ mode is new physics itself. So if anything, D_4 value is very significant for understanding it.

In Section 6, we studied the baryon modes. These modes contain the non-perturbative QCD effects to pollute the possible new physics effect. If we suppose that there is no new physics, we can test the factorization and the pole model, for example. On the other hand, if the experimental result highly differs from these predictions, we should consider the new physics effect. Recently, the lattice gauge theory predicts some B decay processes [25]. We hope that the lattice gauge theory predicts precisely the B meson baryonic decays in near future. If so, we can search for new physics, precisely.

We emphasize that, to discover new physics, it is necessary to determine as many physical quantities as possible, and compare them to the SM predictions. Moreover, it is preferable to be done by the unified form for simplicity, facility, and practicality. This paper will help this process.

References

- [1] Fayyazuddin. Phys. Rev. **D77** 014007 (2008). e-Print: arXiv:0709.3364 [hep-ph]
- [2] Yuval Grossman, Zoltan Ligeti, Enrico Nardi. Phys. Rev. **D55** 2768 (1997). e-Print: hep-ph/9607473
- [3] Dafne Guetta, Enrico Nardi. Phys. Rev. **D58** 012001 (1998). e-Print: hep-ph/9707371
- [4] Particle Data Group (C. Amsler et al.). Phys. Lett. **B667** 1 (2008).
- [5] Hai-Yang Cheng, Chun-Khiang Chua, Shang-Yuu Tsai. Phys. Rev. **D73** 074015 (2006). e-Print: hep-ph/0512335
- [6] J. Kalinowski, Piotr H. Chankowski, Z. Was, M. Worek Acta Phys. Polon. **B36** 3463 (2005). e-Print: hep-ph/0511079

- [7] Piotr H. Chankowski, Jan Kalinowski, Zbigniew Was, Malgorzata Worek. Nucl. Phys. **B713** 555 (2005). e-Print: hep-ph/0412253
- [8] I.I. Bigi and A. I. Sanda. CP Violation, Cambridge University Press, Cambridge, UK 2000.
- [9] So-Young Pi and A. I. Sanda. Ann. Phys. **106** 171 (1977).
- [10] Anjan S. Joshipura, Bhavik P. Kodrani, e-Print: arXiv:0909.0863
- [11] Dafne Guetta, Enrico Nardi. Phys. Rev. **D58** 012001 (1998). e-Print: hep-ph/9707371
- [12] Sacha Davidson, David C. Bailey, Bruce A. Campbell. Z. Phys. **C61** 613 (1994). e-Print: hep-ph/9309310
- [13] Wei Liu, Chong-Xing Yue, Hui-Di Yang. Phys. Rev. **D79** 034008 (2009). e-Print: arXiv:0901.3463
- [14] K.S. Babu, Christopher F. Kolda. Phys. Rev. Lett. **84** 228 (2000). e-Print: hep-ph/9909476
- [15] Zhen-jun Xiao, Lin-xia Lu, Hong-kai Guo, Gong-ru Lu. Chin. Phys. Lett. **16** 88 (1999). e-Print: hep-ph/9903345
- [16] Dafne Guetta, Jesus M. Mira, Enrico Nardi, Phys. Rev. **D59** 034019 (1999), e-Print: hep-ph/9806359
- [17] G. Kaur and M.P. Khanna. Phys. Rev. **D46** 466 (1992).
- [18] M. Jarfi, O. Lazrak, A. Le Yaouanc, L. Oliver, O. Pene, J.C. Raynal. Phys. Rev. **D43** 1599 (1991).
- [19] FOCUS Collaboration, Phys. Lett. **B634** 165 (2006). e-Print: hep-ex/0509042
- [20] E791 Collaboration, Phys. Lett. **B471** 449 (2000), e-Print: hep-ex/9912003
- [21] E791 Collaboration, AIP Conf. Proc. **619** 547 (2002), e-Print: hep-ex/0112025
- [22] CLEO Collaboration, Phys. Rev. **D63** 111102 (2001), e-Print: hep-ex/0011073
- [23] BABAR Collaboration, Phys. Rev. Lett. **96** 241802 (2006), e-Print: hep-ex/0511015.
- [24] Belle Collaboration, e-Print: arXiv:0809.3834.

- [25] G.M. de Divitiis, R. Petronzio, N. Tantalo. Nucl. Phys. **B807** 373 (2009). e-Print: arXiv:0807.2944 ; JLQCD Collaboration. Phys. Rev. **D64** 114505 (2001). e-Print: hep-lat/0106024 ; UKQCD Collaboration. Phys. Rev. **D70** 054501 (2004). e-Print: hep-lat/0404010
- [26] T.Hagiwara, So-Young Pi, A.I.Sanda. Ann. Phys. **106** 134 (1977).

A differential branching ratios for \bar{f}_a and f_b decays

The differential Branching ratio for the process $\bar{f}_a \rightarrow a + \text{anything}$ and $f_b \rightarrow b + \text{anything}$ in \bar{f}_a and f_b rest frame, respectively, are [26];

$$\begin{aligned} \frac{dBr(\bar{f}_a \rightarrow a + \text{anything})}{d^3k_a} &\equiv Br_a \frac{2}{\pi m_a^3 \lambda_a} \left[G_1^a(y_a) + \mathbf{s}^a \cdot \hat{\mathbf{k}}_a G_2^a(y_a) \right], \\ \frac{dBr(f_b \rightarrow b + \text{anything})}{d^3k_b} &\equiv Br_b \frac{2}{\pi m_b^3 \lambda_b} \left[G_1^b(y_b) - \mathbf{s}^b \cdot \hat{\mathbf{k}}_b G_2^b(y_b) \right], \end{aligned} \quad (55)$$

where $G_1^{a,b}(y_{a,b})$ and $G_2^{a,b}(y_{a,b})$ are the functions of $y_{a,b} = 2E_{a,b}/m_{a,b}$, $\lambda_{a,b}$ are defined as

$$\lambda_{a,b} = \int dy_{a,b} y_{a,b}^2 G_1^{a,b}(y_{a,b}), \quad (56)$$

$\hat{\mathbf{k}}_{a,b} = \mathbf{k}_{a,b}/|\mathbf{k}_{a,b}|$ where $k_{a,b}$ are the momentum of the particle a and b , respectively.

We note here that physical vector quantities which we treat in this process are only $\mathbf{s}^{a,b}$ and $\hat{\mathbf{k}}_{a,b}$. The only scalar made by these vector quantities is $\mathbf{s}^{a,b} \cdot \hat{\mathbf{k}}_{a,b}$. So, we can explain the differential branching ratio, Eq. (55) by only two terms which are proportional to $G_1^{a,b}(y_{a,b})$ and $\mathbf{s}^{a,b} \cdot \hat{\mathbf{k}}_{a,b} G_2^{a,b}(y_{a,b})$, respectively.